

Effectiveness of Ventilation Control in a Dry Room with a Heat and Moisture Source

Kwan-Soo Lee*, Kwang-Ok Lim*, Kang-Ho Ahn* and Young-Sick Jung**

Key words: Numerical analysis, Ventilation characteristics

Abstract

The temperature and moisture distributions in a dry room with a heat and moisture source – i.e., workers – are studied numerically by using a standard $k-\epsilon$ turbulence model. In order to evaluate the effectiveness of heat and moisture ventilation inside the room, the heat removal capacity and the moisture exhaust efficiency are introduced. The effectiveness of ventilation control is analyzed by evaluating the temperature and humidity distributions in the room quantitatively. It is found that the mean absolute humidity inside the room is almost constant regardless of the models and the heat generation rates in this study range. This results from the fact that the moisture generation by the workers was relatively small. Through the modification of the design, 40% improvement in critical decay time was achieved.

Nomenclature

C_i : initial moisture concentration [kg/m ³] \bar{C} : instantaneous moisture concentration averaged over the entire room [kg/m ³] C_1, C_2, C_3, C_4 : empirical constants of Eqs. (4), (5) and (6) D_h : hydraulic diameter [m] g : gravitational acceleration [m/s ²] k : turbulent kinetic energy [m ² /s ²] L, H, W : length, height and width [m]	\dot{m} : moisture generation [kg/s] \dot{m}_s : total amount of moisture generation in the room [kg/s] n : normal P : mean pressure [N/m ²] \dot{q} : heat generation per unit area [W/m ²] Q : heat generation per process line [kW] Re : Reynolds number (= $D_h W_{in} / \nu$) T : temperature [°C] u, v, w : x, y, z components of velocity vector [m/s] v_{out}, w_{in} : average velocity at the inlet and outlet [m/s] V : flow rate [m ³ /s] V_0 : volume of the entire room [m ³] x, y, z : space coordinates [m]
---	---

* School of Mechanical Engineering,
Hanyang University, Seoul 133-791, Korea

** Refrigerator Division, LG Electronics Inc.,
Changwon 641-711, Korea

X : absolute humidity [g/kg air]

Greek symbols

α : thermal diffusivity [m^2/s]
 β : volume expansion coefficient [$1/\text{K}$]
 ϕ_m : heat removal capacity [$1/\text{K}$]
 ρ : fluid density [kg/m^3]
 ν : laminar viscosity [m^2/s]
 ν_t : turbulent viscosity [m^2/s]
 ε : turbulent dissipation energy [m^2/s^3]
 $\sigma_k, \sigma_\varepsilon$: empirical parameters of Eqs. (3) and (4)
 σ_T, σ_X : turbulence Prandtl/Schmidt number
 η : moisture exhaust efficiency
 τ : time [s]
 τ_m : non-dimensional ventilation time, $\tau/(V_0/V)$

Subscripts

i, j : tensor index
 m : average
 in, out : inlet and outlet

1. Introduction

A large scale dry room is usually used for mass production of moisture sensitive products. However, the researches on the dry room are in the very beginning stage. Since the dry room has several advantages in terms of productivity compared to the previous inert gas chamber, the dry rooms have been widely employed in recent years. However, one of the disadvantages of the dry room is the high initial investment and operation cost. So, a thorough study on this room is essential to reduce the cost and to optimize the ventilation characteristics.

The previous research related to dry room is very sparse. Theologos et al.⁽¹⁾ developed a

mathematical model for predicting three-dimensional, two-phase, heat and mass transfer inside fluidized-bed dryers. Kiranoudis et al.⁽²⁾ emphasized the spatial homogeneity of air conditions above the product in an industrial batch-type, tray air dryer constructed for drying of several fruits. Lee et al.⁽³⁾ analyzed the ventilation characteristics in a dry room with numerical means.

In this study, the effectiveness of heat and moisture ventilation in a large-scale 3-dimensional dry room has been investigated numerically considering the effects of process line with a heat and moisture source.

2. Theoretical analysis

2.1 Physical model

A dry room that is considered in this study and its design specifications are shown in Fig. 1 (a) and Table 1, respectively. This room has a number of inlets to supply the dry and constant temperature air through the punched plate installed on the ceiling and the twelve outlets that exhaust the air through the sidewalls. Four of the long box-shaped process lines equipped with a conveyor belt are installed along the x -

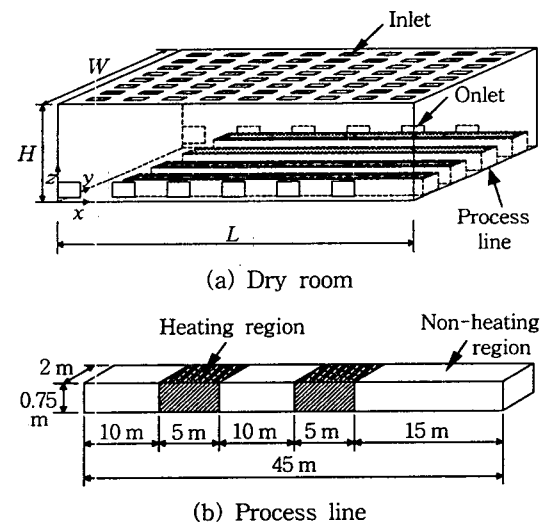


Fig. 1 Schematic diagram of a dry room.

Table 1 Design specifications of a dry room

Contents	Unit	Specifications
Room geometry (L×W×H)	m	51.5×27.63×2.4
Inlet (1.29×1.25 m)	EA	72
Outlet (2.5×0.81 m)	EA	12
Air flow rate	m ³ /min	1760
Ventilation number	No./min	0.5
Workers	Persons	30
Heat generation quantity	kW	10, 20

direction. Fig. 1 (b) shows a process line with heating regions in detail. It is assumed that the uniform heat generation on the heating region of the process line is either 10 kW or 20 kW for each simulation.

For the simplification of the simulation, it is assumed that the workers are the only moisture generation sources in the dry room and they are located near the heating regions. Under this assumption, the moisture generation source regions are matched with the heat sources. The total amount of moisture generation (\dot{m}_s) is calculated by the product of the moisture generation rate by a single adult (0.056 g/s)⁽⁴⁾ and the total number of workers in the dry room. In the simulation it is assumed that 30 workers are present in the dry room. With these assumptions, the total moisture generation in the dry room is 1.68 g/s. In the analysis the ventilation characteristics are investigated at the reference plane located 0.8 m above the floor.

2.2 Governing equations

Since the Reynolds number, defined by the inlet mean velocity and the hydraulic diameter of the inlets, is larger than the order of 10^4 in the dry room, the flow in the dry room is a fully-developed turbulence. To analyze the ventilation characteristics of a physical model, the following assumptions are made:

(1) The flow inside the room is three-dimensional, steady-state, incompressible and tur-

bulent.

(2) All properties are assumed to be constant except the density. The density variation by temperature is considered and calculated using the Boussinesq approximation.

(3) The moisture concentration is assumed to be a passive scalar quantity and, therefore, does not affect the momentum equation. The effects of moisture absorption at the wall surface are negligible.

The mathematical model describing the flow field and moisture distribution within the dry room is expressed by a set of partial differential equations using the standard $k-\epsilon$ turbulence model. The mass and momentum conservation equations can be expressed as follows:

$$\frac{\partial u_i}{\partial x_i} = 0 \quad (1)$$

$$\begin{aligned} \frac{\partial (u_i u_j)}{\partial x_j} = & -\frac{\partial}{\partial x_i} \left(\frac{P}{\rho} + \frac{2}{3} k \right) \\ & + \frac{\partial}{\partial x_j} \left\{ v_t \left(\frac{\partial u_j}{\partial x_j} + \frac{\partial u_i}{\partial x_i} \right) \right\} \\ & + g_i \beta (T - T_{in}) \end{aligned} \quad (2)$$

$$\begin{aligned} \frac{\partial (k u_j)}{\partial x_j} = & \frac{\partial}{\partial x_j} \left(\frac{v_t}{\sigma_k} \frac{\partial k}{\partial x_j} \right) + v_t S - \epsilon \\ & - g_j \beta \frac{v_t}{\sigma_T} \frac{\partial T}{\partial x_j} \end{aligned} \quad (3)$$

$$\begin{aligned} \frac{\partial (\epsilon u_j)}{\partial x_j} = & \frac{\partial}{\partial x_j} \left(\frac{v_t}{\sigma_\epsilon} \frac{\partial \epsilon}{\partial x_j} \right) + \left(C_1 v_t S \right. \\ & \left. - C_2 \epsilon - C_3 g_j \beta \frac{v_t}{\sigma_T} \frac{\partial T}{\partial x_j} \right) \frac{\epsilon}{k} \end{aligned} \quad (4)$$

$$\frac{\partial (T u_j)}{\partial x_j} = \frac{\partial}{\partial x_j} \left\{ \left(a + \frac{v_t}{\sigma_T} \right) \frac{\partial T}{\partial x_j} \right\} + \dot{q} \quad (5)$$

$$\frac{\partial (X u_j)}{\partial x_j} = \frac{\partial}{\partial x_j} \left(\frac{v_t}{\sigma_X} \frac{\partial X}{\partial x_j} \right) \quad (6)$$

where $v_t = C_\mu \frac{k^2}{\epsilon}$, $S = \left(\frac{\partial u_i}{\partial x_i} + \frac{\partial u_j}{\partial x_j} \right) \frac{\partial u_i}{\partial x_j}$, $\sigma_k = 1.0$, $\sigma_\epsilon = 1.3$, $\sigma_T = 0.9$, $\sigma_X = 1.0$, $C_\mu = 0.99$, $C_1 = 1.44$, $C_2 = 1.92$, and $C_3 = 0.7$.

Table 2 Boundary conditions

Inlet	$w_{in} = -0.25 \text{ m/s}$, $k = 0.005 w^2$, $\varepsilon = C_\mu k^{1.5} / (0.5 D_h)$, $X = 0.19 \text{ g/kg air}$
Outlet	$v_{out} = \pm 1.2 \text{ m/s}$, $\frac{\partial k}{\partial n} = 0$, $\frac{\partial \varepsilon}{\partial n} = 0$, $\frac{\partial X}{\partial n} = 0$
Wall	$u, v, w = 0 \text{ m/s}$, $\frac{\partial k}{\partial n} = 0$, $\frac{\partial X}{\partial n} = 0$

2.3 Boundary conditions

The boundary conditions used in this study are listed in Table 2. At the inlets and the outlets of the room, it is assumed that the velocity profile is uniform and the turbulent kinetic energy and its corresponding dissipation rate are the same as Kiranoudis et al.s⁽²⁾ report. At the walls, a non-slip condition and Neumann boundary conditions for the velocity and moisture concentration are applied.

2.4 Numerical analysis

A finite volume method was applied to discretize the governing equations, and the SIMPLER algorithm was used to calculate convection and pressure terms.⁽⁵⁾ The grid dependence test has been performed by changing the number of grid points, i.e. $79 \times 29 \times 19$, $106 \times 34 \times 21$, and $121 \times 41 \times 23$ in x , y , z directions. The grid system adopted in the present model is the non-uniform staggered grids with $106 \times 34 \times 21$ by considering that the changes of the scales of ventilation efficiency are less than 1%. The solution was considered to be converged if the change on the dependent variables in successive iterations was less than 0.001%.

2.5 Heat removal capacity and ventilation efficiency

The ventilation purpose in a dry room is to maintain the constant temperature and humidity during the operation by supplying a dry and constant temperature air. To quantitatively

evaluate the ventilation characteristics, the heat removal capacity and the moisture removal efficiency are introduced.

2.5.1 Heat removal capacity

To evaluate the performance of the different models, the heat removal capacity based on the mean temperature is defined as follows:

$$\phi_m = \frac{1}{T_m - T_{in}} \quad (7)$$

where T_m is the average temperature of the room and T_{in} is the inlet air temperature. Using the heat removal capacity, the performance of a modified dry room can be directly compared.

2.5.2 Moisture removal efficiency

The characteristic of moisture removal is very important in the design of a dry room. The characteristic is also directly related to the ventilation performance. The evaluation of the moisture removal characteristic of a room is made with the moisture concentration in the room as a function of time. The efficiency of moisture removal is defined by the following equation,

$$\eta = 1 - \frac{\bar{C}}{C_i} \quad (8)$$

where \bar{C} and C_i are the instantaneous average moisture concentration and the initial moisture concentration in the room, respectively.

3. Results and discussion

3.1 Analysis of basic model

Fig. 1 shows the basic model used in this study to analyze the flow field, temperature and moisture distributions. Since the room is symmetric, the analysis is done only on the

half section parallel to the $x-z$ plane.

3.1.1 Flow field

The flow pattern in the room is very complicated because of the natural convection due to the heat generation of the process equipment and of the obstacles. The asymmetric distribution of the supply and return ducts causes the leftward flow (x -direction). This flow pattern can be seen in Fig. 2. In this figure the heat generation is not considered

($Q=0$ kW). Fig. 2 (a) shows the strong re-circulations between the supply inlets. Fig. 2 (b) shows the leftward flow pattern.

3.1.2 Temperature and moisture distribution

Fig. 3 shows the temperature distribution for different heat generation rates at the reference plane. It appears that the temperature at the right hand side is slightly lower than that at the left-hand side due to the leftward flow in a room. However, the overall temperature dif-

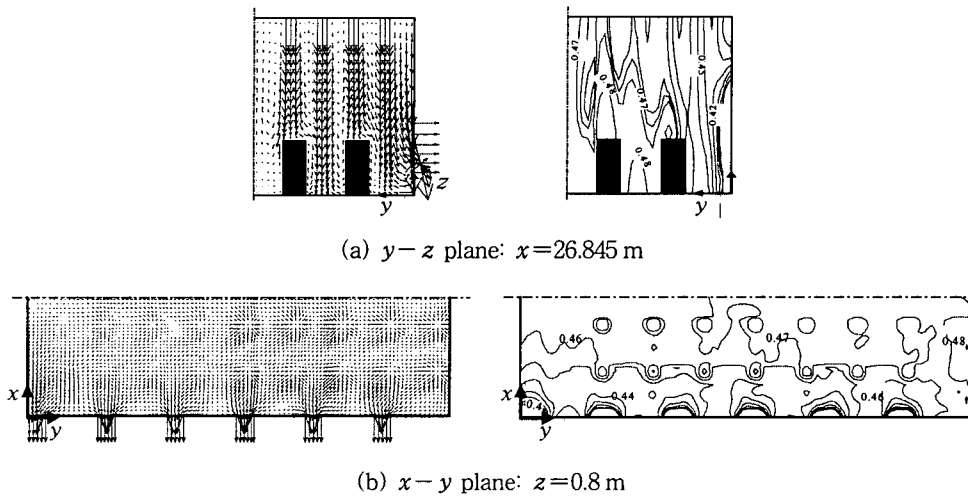


Fig. 2 Velocity vectors and pressure contours in the vertical and horizontal planes ($Q=0$ kW) (pressure unit: N/m^2).

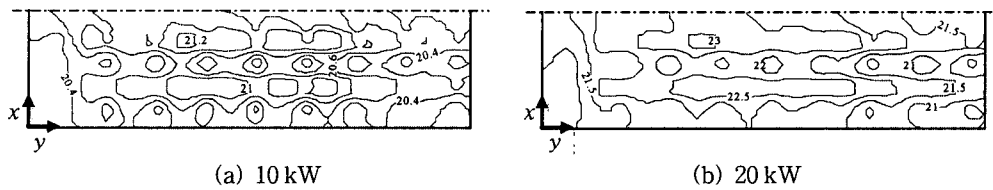


Fig. 3 Temperature distribution for different heat generation rates at the reference plane (unit: $^{\circ}C$).

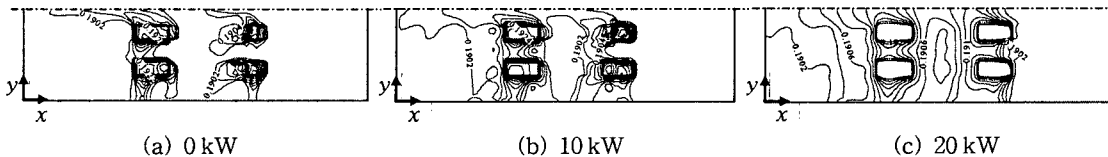


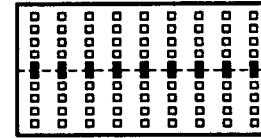
Fig. 4 Absolute humidity distribution for different heat generation rates at the reference plane (unit: g/kg air).

ferences are not so large.

Fig. 4 shows the absolute humidity distribution at the reference plane for three different heat generation rates. In the basic model, the humidity distribution on the left-hand side is slightly higher than that on the right-hand side for all three cases. As mentioned above, the leftward flow causes this skewed distribution. The asymmetric moisture distribution becomes more dominant as the heat generation rate becomes higher. It can be seen in Fig. 4 (c), which shows the high contamination of moisture on the left-hand side. It is caused by the strong buoyancy effect of air on the process line that eventually blocks the incoming air from the inlet. From these moisture distributions, it is expected that moisture removal by ventilation of the basic model is inefficient.

3.2 Analysis of modified model

Since the basic model showed an asymmetric flow and a re-circulation flow near the center plane along the x -direction, the ventilation characteristic is not desirable. To improve the characteristics of moisture ventilation, some modifications in design variables are required in the basic model.



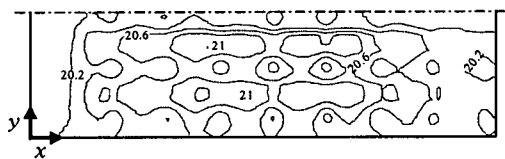
(a) Top view



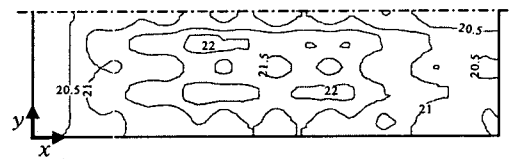
(b) Side view

Fig. 5 Modification of design variables; addition of inlets, outlets (solid blocks) and partition (dashed line).

Fig. 5 shows the modified model with the addition of supply inlets, outlets and a partition. These modifications are proposed to reduce the re-circulation zones and the asymmetric flow pattern. Figs. 6 and 7 show the temperature and moisture distributions, respectively, at the reference plane for different heat generation rates. From the temperature distributions of Figs. 3 and 6, it can be clearly seen that the modified model gives better uniform temperature distribution. This uniformity is mainly achieved by reducing the re-circulation zone and flow asymmetry. The absolute humidity distributions in Fig. 7 shows that high moisture contamination zones have been reduced, compared to that of the basic model shown in



(a) 10 kW



(b) 20 kW

Fig. 6 Temperature distribution for different heat generation rates at the reference plane (unit: $^{\circ}\text{C}$).



(a) 0 kW

(b) 10 kW

(c) 20 kW

Fig. 7 Absolute humidity distribution for different heat generation rates at the reference plane (unit: g/kg air).

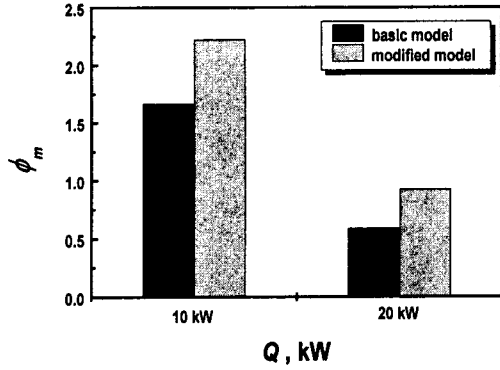


Fig. 8 Heat removal capacity at different heat generation rates.

Fig. 4. The average moisture concentration in the room is about 0.1905 g/kg air, regardless of the model or heat generation rate. This can be explained by the fact that the amount of moisture generated by the workers is too small to affect the ventilation characteristics.

Fig. 8 shows the heat removal capacity as a function of the heat generation rate in the room. It shows that the heat removal capacity of the modified model is higher than that of the basic model, regardless of the heat generation rate. If the heat removal capacity is compared between the basic model and the modified model, the modified model gives a better performance at the high heat generation rate.

Fig. 9 shows the average moisture concentrations in the room at the heat generation rate

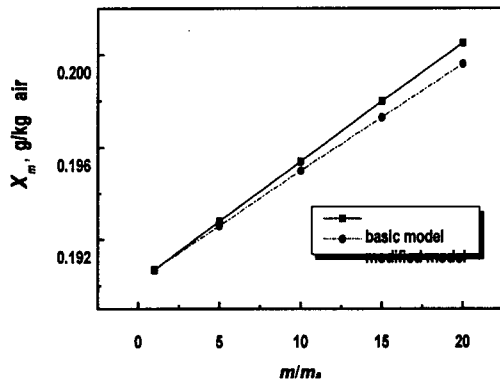


Fig. 9 Average absolute humidity with different moisture generation rates at $Q=20$ kW.

of 20 kW as a function of moisture generation rate. It can be seen that the average moisture concentration in the room is linearly increased as the moisture generation rate increases. The average moisture concentration in the room is not strongly dependent on the models if the moisture generation inside the room is small. However, if the moisture generation in the room increases, then the total moisture in the room is higher for the basic model compared to the modified one. This means that the basic model has a less efficient moisture ventilation characteristic.

3.3 Analysis of ventilation characteristics

The moisture removal efficiency is one of the most effective parameters to analyze the ventilation characteristics in a dry room. Using this parameter, the ventilation characteristic of the dry room is evaluated with the theoretical models, i.e., the plug flow case and the fully mixed flow case.⁽⁶⁾ In the plug flow case, the moisture removal efficiency is defined as follows:

$$\eta = \begin{cases} \tau^*, & 0 \leq \tau^* \leq 1 \\ 1, & \tau^* > 1 \end{cases} \quad (9)$$

where τ^* denotes a non-dimensional ventilation time. Additionally, the fully mixed flow case

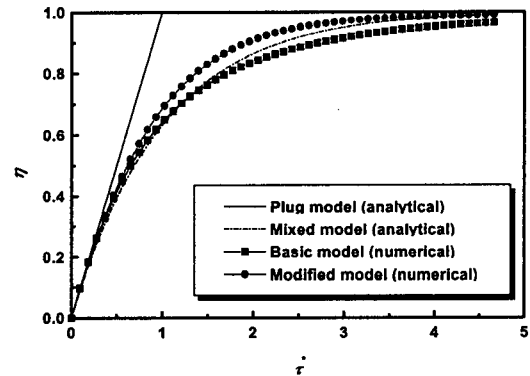


Fig. 10 Moisture removal efficiency as a function of time at $Q=20$ kW.

shows the moisture removal efficiency as follows:

$$\eta = 1 - \exp(-\tau^*) \quad (10)$$

For the comparison of the moisture removal characteristics of each case, 90% removal of the original moisture in the room is defined as a critical decay time.

Fig. 10 shows the moisture removal efficiency as a function of non-dimensional ventilation time. The numerical analysis data for the basic model and the modified model are obtained based on the heat generation rate of 20 kW with Eq. (9). If τ^* is less than about unity, the numerical analysis data for the basic model and the modified model show a better moisture ventilation characteristic than that in the fully developed flow case. It can be explained by the plug flow effect at the beginning of the operation. However, as the time elapses, the incoming air mixes with the aged air. This shows a similar behavior as a fully mixed flow case. So, if a dry room is well designed, the moisture removal efficiency should be higher than the fully mixed flow case. This characteristic is clearly seen in Fig. 10 for the modified model case. If a dry room is not properly designed, the moisture removal efficiency after large τ^* is smaller than that of the fully mixed flow case. The reason is the presence of stagnation zones or re-circulation areas in the dry room. From these results, it can be concluded that, for the best moisture removal efficiency, a dry room should be designed such that the flow in the dry room is similar to the plug flow.

Since the basic model shows an asymmetric and re-circulation flow, it gives the longest critical decay time among the models. However, the modified dry room performs 35% and 40% better than the fully mixed flow case and the basic model, respectively. But its performance is still behind the plug flow case in terms of

the critical decay time.

4. Conclusions

The ventilation characteristics of the dry room are analyzed numerically considering the effect of heat and moisture generation in the room. The effect of modification of the room is also evaluated in terms of the moisture removal characteristics. The flow patterns of the basic model showed some re-circulation zones and asymmetric flow in the room, which results in a less efficient moisture removal characteristic. To improve the moisture removal characteristic, a modification of the basic model is proposed by adding supply inlets on the ceiling, outlets on the sidewalls and a partition at the middle. These modifications provide a more uniform flow pattern and better heat and moisture removal characteristics. The average moisture concentration in the room is almost constant at 0.1905 g/kg air, regardless of the heat generation rate and the modification of the room. However, the modified model showed a better performance than the basic model in terms of the moisture removal characteristic, especially at a high heat generation condition. The modified model also showed a better performance by 40% in terms of the critical decay time than the basic model.

Acknowledgments

This research was supported by the Center of Innovative Design Optimization Technology (iDOT), Korea Science and Engineering Foundation (KOSEF) and the Brain Korea 21 Project.

References

1. Theologos, K. N., Maroulis, Z. B. and Markatos, N. C., 1997, Simulation of Transport Dynamics in Fluidized-Bed Dryers, *Drying Technology*, 15(5), pp. 1265-1291.

2. Kiranoudis, C. T., Karathanos, V. T. and Markatos, N. C., 1999, Computational Fluid Dynamics of Industrial Batch Dryers of Fruits, *Drying Technology*, 17(1-2), pp. 1-25.
3. Lee, K. S., Lim, K. O., Ahn, K. H. and Jung, Y. S., 2001, Numerical Analysis of Moisture Ventilation in a Lithium Ion Battery Manufacturing Dry Room, *Drying Technology*, Vol. 19, No. 3, pp. 455-470.
4. Harris, N. C., 1983, *Modern Air Conditioning Practice*, 3rd ed., McGraw-Hill, New York.
5. Patankar, S. V., 1980, *Numerical Heat Transfer and Fluid Flow*, McGraw-Hill.
6. Lage, J. L., Bejan, A. and Anderson, R., 1991, Efficiency of Transient Contaminant Removal from a Slot Ventilated Enclosure, *Int. J. Heat Mass Transfer*, 34(10), pp. 2603-2615.